

# DESINGULARIZATION IN COMPUTATIONAL APPLICATIONS AND EXPERIMENTS

ANNE FRÜHBIS-KRÜGER

**ABSTRACT.** After briefly recalling some computational aspects of blowing up and of representation of resolution data common to a wide range of desingularization algorithms (in the general case as well as in special cases like surfaces or binomial varieties), we shall proceed to computational applications of resolution of singularities in singularity theory and algebraic geometry, also touching on relations to algebraic statistics and machine learning. Namely, we explain how to compute the intersection form and dual graph of resolution for surfaces, how to determine discrepancies, the log-canonical threshold and the topological Zeta-function on the basis of desingularization data. We shall also briefly see how resolution data comes into play for Bernstein-Sato polynomials, and we mention some settings in which desingularization algorithms can be used for computational experiments. The latter is simply an invitation to the readers to think themselves about experiments using existing software, whenever it seems suitable for their own work.

## 1. INTRODUCTION

This article originated from the notes of an invited talk at the Clay Mathematics Institute summer school on "The Resolution of Singular Algebraic Varieties" in Obergurgl, Austria, 2012. As the whole school was devoted to desingularization, the focus in this particular contribution is on applications and on practical aspects. A general knowledge of resolution of singularities and different approaches to this task is assumed and can be acquired from other parts of this proceedings volume. The overall goal of this article is to give readers a first impression of a small choice of applications and point them to good sources for further reading on each of the subjects. A detailed treatment of each of the topics would fill an article by itself and is thus beyond the scope here.

One focus here is on the practical side. To this end, we first revisit desingularization algorithms in section 2 and have a closer look at the representation of resolution data: as a consequence of the heavy use of blowing up, the data is distributed over a rather large number of charts which need to be glued appropriately. Glueing, however, only describes the theoretical side of the process; from the practical point of view, it is closer to an identification of common points in charts.

In section 3 we focus on applications needing different amounts of resolution data. Using an abstract resolution of singularities only, the computation of the intersection form and dual graph of the resolution for surface singularities requires the smallest amount of data. For determining discrepancies and the log-canonical threshold, we already need an embedded resolution which is also required for the

---

partially supported by DFG priority program SPP 1489 'Algorithmic and Experimental Methods in Algebra, Geometry and Number Theory'.

third application, the computation of the topological zeta function.

In the rather short last section, we only sketch two settings in which one might want to use algorithmic desingularization as an experimental tool: the roots of the Bernstein-Sato polynomial and resolution experiments in positive characteristic. This last part is not intended to provide actual research projects. It is only intended to help develop a feeling for settings in which experiments can be helpful. All parts of the article are illustrated by the same simple example which is desingularized using a variant of Villamayor's algorithm available in SINGULAR. Based on this resolution data, all further applications are also accompanied by the corresponding SINGULAR-code. The SINGULAR code is not explained in detail, but hints and explanations on the appearing commands and their output are provided as comments in the examples. To further familiarize with the use of SINGULAR in this context, we recommend that the readers try out the given session themselves and use the built-in manual of SINGULAR to obtain further information on the commands (e.g.: `help resolve`; returns the help page of the command `resolve`).

I would like to thank the organizers of the summer school for the invitation. Insights from conversations with many colleagues have contributed to the content of these notes. In particular, I would like to thank Herwig Hauser, Gerhard Pfister, Ignacio Luengo, Alejandro Melle, Frank-Olaf Schreyer, Wolfram Decker, Hans Schönemann, Duco van Straten, Nobuki Takayama, Shaowei Lin, Frank Kiraly, Bernd Sturmfels, Zach Teitler, Nero Budur, Rocio Blanco and Santiago Encinas for comments, of which some led to applications explained here and some others helped seeing the applications in broader context. For reading earlier versions of this article and many helpful questions on the subject of this article, I am indebted to Frithjof Schulze and Bas Heijne.

## 2. DESINGULARIZATION FROM THE COMPUTATIONAL SIDE

Before turning toward applications of resolution of singularities, we need to review certain aspects of algorithmic desingularization to understand the way in which the computed resolution data is represented. Although there are various settings in which different resolution algorithms have been created, we may discern three main approaches suitable for the purposes of this article: the algorithms based on Hironaka's proof in characteristic zero in any dimension (see e.g. [8], [5], [13]), the algorithms for binomial and toric ideals (see e.g. [15], [7], [6]) and the algorithms for 2-dimensional varieties and schemes (such as [2] – based on [19] – or [24]).<sup>1</sup> The algorithms of the first kind of approach involve embedded desingularization, i.e. they blow up a smooth ambient space and consider the strict transform of the variety and the exceptional divisors inside the new ambient space. The algorithms for 2-dimensional varieties on the other hand, do not consider the embedded situation, but blow up the variety itself and consider exceptional divisors inside the blown up variety.

It would be beyond the scope of this article to cover all these algorithms in depth, but they all have certain ingredients in common. In the first two situations,

---

<sup>1</sup>Of course this list of approaches is far from exhaustive, but it is intended to narrow down our scope to those which lead to similar forms of resolution data allowing similar applications later on.

a desingularization is achieved by finite sequences of blow-ups at suitable non-singular centers. The differences between these algorithms then lie in the choice of center, which is the key step of each of these, but does not affect the structure of the practical representation of resolution data. For the third class of algorithms, blow-ups are not the only tool, but are combined with other tools, in particular normalization steps. However, the exceptional divisors to be studied arise from blow-ups and additionally only require proper tracing through the normalization steps if necessary. Therefore the technique to focus on in this context is blowing up; more precisely blowing up at non-singular centers.

**2.1. Blowing up – the computational side.** Let us briefly recall the definition of blowing up, as it can be found in any textbook on algebraic geometry (e.g. [16]), before explaining its computational side:

**Definition 1.** *Let  $X$  be a scheme and  $Z \subset X$  a subscheme corresponding to a coherent ideal sheaf  $\mathcal{I}$ . The blowing up of  $X$  with center  $Z$  is*

$$\pi : \bar{X} := \text{Proj}\left(\bigoplus_{d \geq 0} \mathcal{I}^d\right) \longrightarrow X.$$

*Let  $Y \xrightarrow{i} X$  be a closed subscheme and  $\pi_1 : \bar{Y} \longrightarrow Y$  the blow up of  $Y$  along  $i^{-1}\mathcal{I}\mathcal{O}_Y$ . Then the following diagram commutes*

$$\begin{array}{ccc} \bar{Y} & \hookrightarrow & \bar{X} \\ \pi_1 \downarrow & & \downarrow \pi \\ Y & \hookrightarrow & X \end{array}$$

*$\bar{Y}$  is called the strict transform of  $Y$ ,  $\pi^*(Y)$  the total transform of  $Y$ .*

To make  $\bar{X}$  accessible to explicit computations of examples in computer algebra systems, it should best be described as the zero set of an ideal in a suitable ring. We shall assume now for simplicity of presentation that  $X$  is affine because schemes are usually represented in computer algebra systems by means of affine covers. So we are dealing with the following situation:  $J = \langle f_1, \dots, f_m \rangle \subset A$  is the vanishing ideal of the center  $Z \subset X = \text{Spec}(A)$  and the task is to compute

$$\text{Proj}\left(\bigoplus_{d \geq 0} J^d\right).$$

To this end, we consider the canonical graded  $A$ -algebra homomorphism

$$\Phi : A[y_1, \dots, y_m] \longrightarrow \bigoplus_{n \geq 0} J^n t^n \subset A[t]$$

defined by  $\Phi(y_i) = t f_i$ . The desired object  $\bigoplus_{d \geq 0} J^d$  is then isomorphic to

$$A[y_1, \dots, y_m] / \ker(\Phi)$$

or from the more geometric point of view  $V(\ker(\Phi)) \subset \text{Spec}(A) \times \mathbb{P}^{m-1}$ .

The computation of the kernel in the above considerations is a standard basis computation and further such computations arise during the calculation of suitable centers in the different algorithms. Moreover, each blowing up introduces a further set of new variables as we have just seen and desingularization is hardly

ever achieved with just one or two blow-ups – usually we are seeing long sequences thereof. The performance of standard bases based algorithms, on the other hand, is very sensitive to the number of variables as its complexity is doubly exponential in this number. Therefore it is vital from the practical point of view to pass from the  $\mathbb{P}^{m-1}$  to  $m$  affine charts and pursue the resolution process further in each of the charts<sup>2</sup>; consistency of the choice of centers does not pose a problem at this stage as this follows from the underlying desingularization algorithm. Although this creates an often very large tree of charts with the final charts being the leaves and although it postpones a certain part of the work, this approach has a further important advantage: it allows parallel computation by treating several charts on different processors or cores at the same time.

As a sideremark, we also want to mention the computation of the transforms, because they appeared in the definition cited above; for simplicity of notation we only state the affine case. Without any computational effort, we obtain the exceptional divisor as  $I(H) = J\mathcal{O}_{\overline{X}}$  and the total transform  $\pi^*(I) = I\mathcal{O}_{\overline{X}}$  for a subvariety  $V(I)$  in our affine chart. The strict transform is then obtained by a saturation, i.e. an iteration of ideal quotients until it stabilizes:  $I_{\overline{V(I)}} = (\pi^*(I) : I(H)^\infty)$ ; for the weak transform, the iteration stops before it stabilizes, namely at the point where multiplying with the ideal of the exceptional divisor gives back the result of the previous iteration step for the last time. These ideal quotient computations are again based on standard bases.

**2.2. Identification of Points in Different Charts.** As we have just seen, it is more useful for the overall performance to pass to affine charts after each blow-up, even though this leads to an often rather large tree of charts. As a consequence, it is not possible to directly work with the result without any preparation steps, namely identifying points which are present in more than one chart – a practical step equivalent to the glueing of the charts. This is of particular interest for the identification of exceptional divisors which are present in more than one chart.

For the identification of points in different charts, we need to pass through the tree of charts – from one final chart all the way back to the last common ancestor of the two charts and then forward to the other final chart. As blowing up is an isomorphism away from the center, this step does not pose any problems as long as we do not need to identify points lying on an exceptional divisor which was not yet created in the last common ancestor chart. In the latter case, however, we do not have a direct means of keeping track of points originating from the same point of the center. The way out of this dilemma is a representation of points on the exceptional divisor as the intersection of the exceptional divisor with an auxilliary variety not contained in the exceptional divisor. More formally, the following simple observation from commutative algebra can be used:

**Remark 2.** *Let  $I \subset K[x_1, \dots, x_n]$  be a prime ideal,  $J \subset K[a_1, \dots, x_n]$  another ideal such that  $I + J$  is equidimensional and  $\text{ht}(I) = \text{ht}(I + J) - r$  for some integer  $0 < r < n$ . Then there exist polynomials  $p_1, \dots, p_r \in I + J$  and a polynomial*

---

<sup>2</sup>In practice, it is very useful to discard all charts not appearing in any other chart and not containing any information which is relevant for the desired application.

$f \in K[x_1, \dots, x_n]$  such that

$$\sqrt{I+J} = \sqrt{(I + \langle p_1, \dots, p_r \rangle) : f}.$$

At first glance, this seems non-constructive, but it turns out to be applicable in a very convenient way: In our situation,  $I$  describes the intersection of exceptional divisors containing the point (or subvariety  $V(J)$ ) in question. As any sufficiently general set of polynomials  $p_1, \dots, p_r \in J \setminus (I \cap J)$  with correct height of  $I + \langle p_1, \dots, p_r \rangle$  will serve our purpose and so will any  $f$  that excludes all extra components of  $I + \langle p_1, \dots, p_r \rangle$ , we have sufficient freedom of choice of  $p_1, \dots, p_r, f$  such that none of these is contained in any further exceptional divisor whose moment of birth has to be crossed during the blowing down process.

Given this means of identification of points, we can now also identify the exceptional divisors or, more precisely, the centers leading to the respective exceptional divisors. To avoid unnecessary comparisons between centers in different charts, we can a priori rule out all comparisons involving centers lying in different exceptional divisors. If the desingularization is controlled by an invariant as in [8], [5] or [7], we can also avoid comparisons with different values of the controlling invariant, because these cannot give birth to the same exceptional divisor either.

**Example 3.** *To illustrate the explanations given so far and to provide a practical example to be used for all further applications, we now consider an isolated surface singularity of type  $A_4$  at the origin. We shall illustrate this example using the computer algebra system SINGULAR ([11]).*

```
> // load the appropriate libraries for resolution of singularities and
> // applications thereof
> LIB"resolve.lib";
> LIB"reszeta.lib";
> LIB"resgraph.lib";

> // define the singularity
> ring R=0,(x,y,z),dp;
> ideal I=x5+y2+z2;           // an A4 surface singularity

> // compute a resolution of the singularity (Villamayor-approach)
> list L=resolve(I);
> size(L[1]);                 // final charts
6
> size(L[2]);                 // all charts
11
> def r9=L[2][9];             // go to chart 9
> setring r9;
> showB0(B0);                 // show data in chart 9

==== Ambient Space:
_[1]=0

==== Ideal of Variety:
_[1]=x(2)^2+y(0)+1
```

```

==== Exceptional Divisors:
[1]:
  _[1]=1
[2]:
  _[1]=y(0)
[3]:
  _[1]=1
[4]:
  _[1]=x(1)

==== Images of variables of original ring:
_[1]=x(1)^2*y(0)
_[2]=x(1)^5*x(2)*y(0)^2
_[3]=x(1)^5*y(0)^2
> setring R;                                // go back to old ring

```

*This yields a total number of 11 charts of which 6 are final charts. All blow-ups have zero-dimensional centers except the two line blow-ups leading from chart 6 to charts 8 and 9 and from chart 7 to charts 10 and 11. As it would not be very useful to reproduce all data of this resolution here, we show the total tree of charts as illustration 3 and give the content of chart 9 as an example:*

*strict transform*<sup>3</sup>:  $V(x_2^2 + y_0 + 1)$   
*exceptional divisors*:  $V(y_0)$  from 2nd blow-up  
                            $V(x_1)$  from last blow-up  
*images of variables of original ring*:

$$\begin{aligned} x &\longmapsto x_1^2 y_0 \\ y &\longmapsto x_1^5 x_2 y_0^2 \\ z &\longmapsto x_1^5 y_0^2 \end{aligned}$$

*For example, the exceptional divisor originating from the last blow-up leading to chart 9 needs to be compared to the exceptional divisor originating from the last blow-up leading to chart 10. To this end, one needs to consider the centers computed in charts 6 and 7 which turn out to be the intersection of the exceptional divisors labeled 2 and 3, if one considers the output of the resolution process in detail<sup>4</sup>. Therefore the last exceptional divisors in charts 9 and 10 coincide. This identification is implemented in SINGULAR and can be used in the following way:*

```

> // identify the exceptional divisors
> list coll=collectDiv(L);
> coll[1];
0,0,0,0, // no exc. div. in chart 1
1,0,0,0, // first exc. div. is first in chart 2
1,0,0,0, // .....
1,2,0,0, // data too hard to read, better
0,2,0,0, // use command below to create figure 1

```

<sup>3</sup>Weak and strict transform coincide for hypersurfaces.

<sup>4</sup>We encourage the reader to verify this by typing the above sequence of commands into SINGULAR and then exploring the data in the different charts.

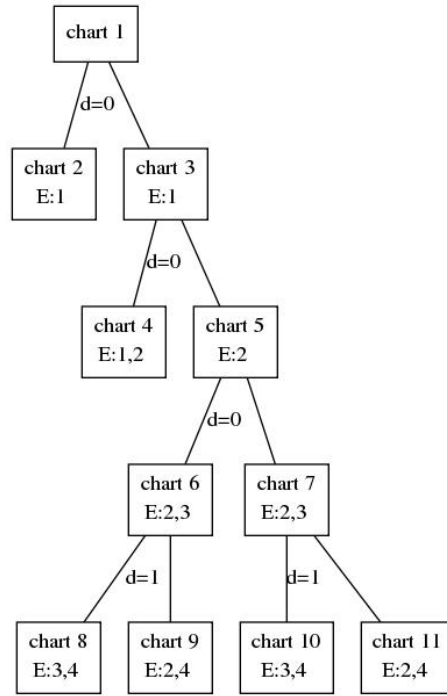


FIGURE 1. Tree of charts of an embedded desingularization of an  $A_4$  surface singularity. The numbers given in the second line in each chart are the labels of the exceptional divisors visible in the respective chart. The numbers stated as  $d = 0$  or  $d = 1$  state the dimension of the center of the corresponding blow-up. Charts providing only data which is also present in other charts are not shown.

0,2,3,0,  
 0,2,3,0,  
 0,0,3,4,  
 0,2,0,4,  
 0,0,3,4,  
 0,2,0,4

```
> //present the tree of charts as shown in figure 1
> ResTree(L, coll[1]);
```

### 3. APPLICATIONS OF RESOLUTION OF SINGULARITIES

The applications we present in this section originate from different subfields of mathematics ranging from algebraic geometry to singularity theory and  $D$ -modules. For each application we shall revisit our example from the previous section and also show how to perform the corresponding computation using SINGULAR.

**3.1. Intersection Form and Dual Graph of Resolution.** Given a resolution of an isolated surface singularity, we want to compute the intersection matrix of

the exceptional divisors. This task does not require an embedded resolution of singularities, only an abstract one. Given such a desingularization, it can then be split up into 3 different subtasks:

- (1) computation of the intersections  $E_i.E_j$  for exceptional curves  $E_i \neq E_j$
- (2) computation of the self-intersection numbers  $E_i^2$  for the exceptional curves  $E_i$
- (3) representation of the result as the dual graph of the resolution

If the given resolution, is not an abstract one, but an embedded one - like the result of Villamayor's algorithm - we need to add a preliminary step

- (0) determine an abstract resolution from an embedded one. <sup>5</sup>

Although the definition of intersection numbers of divisors on surfaces can be found in many textbooks on algebraic geometry (e.g. in [16], V.1), we give a brief summary of the used properties for readers' convenience:

**Definition 4.** Let  $D_1, D_2$  be divisors in general position<sup>6</sup> on a non-singular surface  $X$ . Then the intersection number of  $D_1$  and  $D_2$  is defined as

$$D_1.D_2 := \sum_{x \in D_1 \cap D_2} (D_1.D_2)_x$$

where  $(D_1.D_2)_x$  denotes the intersection multiplicity of  $D_1$  and  $D_2$  at  $x$ .

**Lemma 5.** For any divisors  $D_1$  and  $D_2$  on a non-singular surface  $X$ , there exist divisors  $D'_1$  and  $D'_2$ , linearly equivalent to  $D_1$  and  $D_2$  respectively, such that  $D'_1$  and  $D'_2$  are in general position.

**Lemma 6.** Intersection numbers have the following basic properties:

- (a) For any divisors  $C$  and  $D$ :  $C.D = D.C$ .
- (b) For any divisors  $C$ ,  $D_1$  and  $D_2$ :  $C.(D_1 + D_2) = C.D_1 + C.D_2$
- (c) For any divisors  $C$ ,  $D_1$  and  $D_2$ , such that  $D_1$  and  $D_2$  are linearly equivalent:  $C.D_1 = C.D_2$ .

At this point, we know what we want to compute, but we have to take care of another practical problem before proceeding to the actual computation which is then a straight forward calculation of the intersection numbers of exceptional curves  $E_i \neq E_j$ . The practical problem is that computations in a computer algebra system usually take place in polynomial rings over the rationals or algebraic extensions thereof. So we easily achieve a decomposition of the exceptional divisor into  $\mathbb{Q}$ -irreducible components, but we need to consider  $\mathbb{C}$ -irreducible components to obtain the intersection matrix we expect from the theoretical point of view. To this end, passing to suitable extensions of the ground field may be necessary – be it explicitly by introducing a new variable and a minimal polynomial (slowing down subsequent computations) or implicitly by taking into account the number of components over  $\mathbb{C}$  for each  $\mathbb{Q}$ -component.

**Example 7.** Revisiting our example of a desingularization of an  $A_4$  surface singularity, we first need to pass to an abstract resolution.

<sup>5</sup>This is achieved by canceling all trailing blow-ups in our tree of charts which are unnecessary for the non-embedded case. Then the intersection of the remaining exceptional divisors with the strict transform yields the exceptional locus of the non-embedded resolution.

<sup>6</sup> $D_1$  and  $D_2$  are in general position, if the intersection  $\text{Supp}(D_1) \cap \text{Supp}(D_2)$  is either empty or a finite set of points.



```

\\ compute part of the tree of charts relevant for abstract resolution
> abstractR(L)[1];
    0,1,0,1,1,0,0,0,0,0,0    //final charts are 2,4,5
> abstractR(L)[2];
    0,0,0,0,0,1,1,1,1,1,1    //charts 6 and higher are irrelevant
                                //for non-embedded case

```

So we only see 2 exceptional divisors in the final charts, the ones labeled 1 and 2 (cf. figure 3). But looking at the charts in more detail, we would see e.g. in chart 4 that the first divisor is given by  $V(y_2, y_0^2 + 1)$  and the second one by  $V(x_2, y_0^2 + 1)$ . So each of these has two  $\mathbb{C}$ -irreducible components. Considering these  $\mathbb{C}$ -components, we can obtain the following intersection data (seeing two of the intersections directly in chart 4 and the remaining one in chart 5):

$$\begin{pmatrix} * & 0 & 1 & 0 \\ 0 & * & 0 & 1 \\ 1 & 0 & * & 1 \\ 0 & 1 & 1 & * \end{pmatrix}$$

Hence only the self-intersection numbers – marked as \* in the matrix – are still missing.

For the self-intersection numbers of the exceptional curves, we need to make use of another property of divisors in the context of desingularization:

**Lemma 8.** *Let  $\pi : \tilde{X} \rightarrow X$  be a resolution of singularities of a surface  $X$ . Let  $D_1$  be a divisor on  $\tilde{X}$  all of whose components are exceptional curves of  $\pi$  and let  $D_2$  be a divisor on  $X$ , then*

$$\pi^*(D_2).D_1 = 0.$$

Denoting by  $E_1, \dots, E_s$  the  $\mathbb{C}$ -irreducible exceptional curves, we can hence consider a linear form  $h : X \rightarrow \mathbb{C}$  passing through the only singular point of  $X$  and the divisor  $D$  defined by it. We then know

$$\pi^*(D) = \sum_{i=1}^s c_i E_i + H$$

where  $H$  denotes the strict transform of  $D$  and the  $c_i$  are suitable integers. From the lemma we additionally know that

$$0 = \pi^*(D).E_j = \sum_{i=1}^s c_i E_i.E_j + H.E_j \quad \forall 1 \leq j \leq s$$

where all intersection numbers are known or directly computable in each of the equations except the self-intersection numbers  $E_j.E_j$  which we can compute in this way. For the dual graph of the resolution, each divisor is represented by a vertex (those with self-intersection -2 are unlabeled, the other ones labeled by their self-intersection number), each intersection is represented by an edge linking the two vertices corresponding to the intersecting exceptional curves.

**Example 9.** *The computation of the intersection form is implemented in SINGULAR and can be used as follows:*

```

> // intersection matrix of exceptional curves
> // (no previous abstractR is needed, this is done automatically)

```

```

> // in the procedure intersectionDiv)
> list iD=intersectionDiv(L);
> iD[1];
-2,0,1,0,
0,-2,0,1,
1,0,-2,1,
0,1,1,-2

```

```

> // draw the dual graph of the resolution
InterDiv(iD[1]);

```

*This yields the expected intersection matrix (as entry  $iD[1]$  of the result)*

$$\begin{pmatrix} -2 & 0 & 1 & 0 \\ 0 & -2 & 0 & 1 \\ 1 & 0 & -2 & 1 \\ 0 & 1 & 1 & -2 \end{pmatrix}$$

*and the dual graph of the resolution which is just the Dynkin diagram of the  $A_4$  singularity.*

**3.2. Discrepancies and Log-canonical Threshold.** In contrast to the last task, which only required an abstract resolution of the given surface singularity, the task of computing (log-)discrepancies and the log-canonical threshold requires embedded desingularization (or principalization of ideals). This is provided by Villamayor's algorithm. As before we first recall the definitions and some basic properties (see e.g. [25] for a direct and accessible introduction to the topic). To keep the exposition as short as possible and the considerations directly accesible to explicit computation, we restrict our treatment here to the case of a singular affine variety.

**Definition 10.** *Let  $f \in \mathbb{C}[x_1, \dots, x_n]$  be a non-zero polynomial defining a hypersurface  $V$  and let  $\pi : X \rightarrow \mathbb{C}^n$  be an embedded resolution of  $V$ . Denote by  $E_i$ ,  $i \in I$ , the irreducible components of the divisor  $\pi^{-1}(f^{-1}(0))$ . Let  $N(E_j)$  denote the multiplicity of  $E_j$ ,  $j \in J$  in the divisor of  $f \circ \pi$  and let  $\nu(E_j) - 1$  be the multiplicity of  $E_j$  in the divisor  $K_{X/\mathbb{C}^n} = \pi^*(dx_1 \wedge \dots \wedge dx_n)$ . Then the log-discrepancies of the pair  $(\mathbb{C}^n, V)$  w.r.t.  $E_j$ ,  $j \in J$ , are*

$$a(E_j; \mathbb{C}^n, V) := \nu(E_j) - N(E_j).$$

*The minimal log discrepancy of the pair  $(\mathbb{C}^n, V)$  along a closed subset  $W \subset \mathbb{C}^n$  is the minimum over the log-discrepancies for all  $E_j$  with  $\pi(E_j) \subset W$ , i.e. originating from (sequences of) blow-ups with centers in  $W$ . The log-canonical threshold of the pair  $(\mathbb{C}^n, V)$  is defined as*

$$lct(\mathbb{C}^n, V) = \inf_{j \in J} \frac{\nu(E_j)}{N(E_j)}.$$

**Remark 11.** *The above definition of log-discrepancies and log-canonical threshold holds in a far broader context. Allowing more general pairs  $(Y, V)$  it is also the basis for calling a resolution of singularities log-canonical, if the minimal log discrepancy of the pair along all of  $Y$  is non-negative, and log-terminal, if it is positive.*

As we already achieved an identification of exceptional divisors in a previous section, the only computational task here is the computation of the multiplicities

$N(E_i)$  and  $\nu(E_i)$ . The fact that we might be dealing with  $\mathbb{Q}$ -irreducible, but  $\mathbb{C}$ -reducible  $E_i$  does not pose any problem here, because we can easily check that the respective multiplicities coincide for all  $\mathbb{C}$ -components of the same  $\mathbb{Q}$ -component. To compute these multiplicities from the resolution data in the final charts (i.e. without moving through the tree of charts), we can determine  $N(E_i)$  by finding the highest exponent  $j$  such that  $I(E_j)^j : J$  is still the whole ring where  $J$  denotes the ideal of the total transform of the original variety. To compute the  $\nu(E_i)$  we can use the same approach, but taking into account the appropriate Jacobian determinant.

**Example 12.** *We now simply continue our SINGULAR session on the basis of the data already computed in the previous examples*

```
> // identify exceptional divisors (embedded case)
> list iden=prepEmbDiv(L);

> // multiplicities N(Ei)
> intvec cN=computeN(L,iden);
> cN;           // last integer is strict transform
2,4,5,10,1

> // multiplicities v(Ei)
> intvec cV=computeV(L,iden);
> cV;           // last integer is strict transform
3,5,7,12,1

> // log-discrepancies
> discrepancy(L);
0,0,1,1

> // compute log-canonical threshold
> // as an example of a loop in Singular
> number lct=number(cV[1])/number(cN[1]);
> number lcttemp;
> for (int i=1; i < size(cV); i++)
> {
>   lcttemp=number(cV[i])/number(cN[i]);
>   if(lcttemp < lct)
>   {
>     lct=lcttemp;
>   }
> }
> lct;
6/5
```

The log-canonical threshold, in particular, is a very important invariant which appears in many different contexts, ranging from a rather direct study of properties of pairs to the study of multiplier ideals (cf. [22]), to motivic integration or to Tian's  $\alpha$ -invariant which provides a criterion for the existence of Kähler-Einstein metrics (cf. [28]).

A real analogue to the log-canonical threshold, the real log-canonical threshold appears when applying resolution of singularities in the real setting [26]. In algebraic statistics, more precisely in model selection in Bayesian statistics, desingularization plays an important role in understanding singular models by monomializing the so-called Kullback-Leibler function at the true distribution. In this context the real log-canonical threshold is then used to study the asymptotics of the likelihood integral.[23]. It also appears in singular learning theory as the learning coefficient.

**3.3. Topological Zeta Function.** Building upon the multiplicities of  $N(E_i)$  and  $\nu(E_i) - 1$  of exceptional curves appearing in  $f \circ \pi$  and  $K_{X/\mathbb{C}^n} = \pi^*(dx_1 \wedge \dots \wedge dx_n)$  which already appeared in the previous section, we can now define and compute the topological Zeta-function. As before, we first recall the definitions and properties (see e.g. [12]) and then continue with the computational aspects – listing the corresponding SINGULAR commands in the continued example of an  $A_4$  surface singularity.

**Definition 13.** Let  $f \in \mathbb{C}[x_1, \dots, x_n]$  be a non-zero polynomial defining a hypersurface  $V$  and let  $\pi : X \rightarrow \mathbb{C}^n$  be an embedded resolution of  $V$ . Denote by  $E_i$ ,  $i \in I$ , the irreducible components of the divisor  $\pi^{-1}(f^{-1}(0))$ . To fix notation, we define for each subset  $J \subset I$

$$E_J := \bigcap_{j \in J} E_j \text{ and } E_J^* := E_J \setminus \bigcup_{j \notin J} E_{J \cup \{j\}}$$

and denote for each  $j \in I$  the multiplicity of  $E_j$  in the divisor of  $f \circ \pi$  by  $N(E_j)$ . We further set  $\nu(E_j) - 1$  to be the multiplicity of  $E_j$  in the divisor  $K_{X/\mathbb{C}^n} = \pi^*(dx_1 \wedge \dots \wedge dx_n)$ . In this notation the topological Zeta-function of  $f$  is

$$Z_{\text{top}}^{(d)}(f, s) := \sum_{\substack{J \subset I \text{ s.th.} \\ d | N(E_j) \forall j \in J}} \chi(E_J^*) \prod_{j \in J} (\nu(E_j) + N(E_j)s)^{-1} \in \mathbb{Q}(s).$$

Intersecting the  $E_J^*$  with the preimage of zero in the above formula leads to the local topological Zeta-function

$$Z_{\text{top},0}^{(d)}(f, s) := \sum_{\substack{J \subset I \text{ s.th.} \\ d | N(E_j) \forall j \in J}} \chi(E_J^* \cap \pi^{-1}(0)) \prod_{j \in J} (\nu(E_j) + N(E_j)s)^{-1} \in \mathbb{Q}(s).$$

(The local and global topological Zeta-function are independent of the choice of embedded resolution of singularities of  $V$ .)

Here, it is again important to observe that in the above context the irreducible components are taken over  $\mathbb{C}$ , while practical calculations usually take place over  $\mathbb{Q}$  and further passing to components taken over  $\mathbb{C}$  is rather expensive. The following lemma shows that considering  $\mathbb{Q}$ -irreducible components already allows the computation of the  $\zeta$ -function:

**Lemma 14.** Let  $D_l$ ,  $l \in L$ , be the  $\mathbb{Q}$ -irreducible components of the divisor  $\pi^{-1}(f^{-1}(0))$ . For each subset  $J \subset L$  define  $D_J$  and  $D_J^*$  as above. Then the topological (global and local) Zeta-function can be computed by the above formulae using the  $D_J$  and  $D_J^*$  instead of the  $E_J$  and  $E_J^*$ .

As we already identified the exceptional divisors and computed the multiplicities  $N(E_i)$  and  $\nu(E_i)$ , the only computational data missing is the Euler characteristic

of the exceptional components in the final charts. If the intersection of exceptional divisors is zero-dimensional, this is just a matter of counting points using the identification of points in different charts. For 1-dimensional intersections the Euler characteristic can be computed using the geometric genus of the curve (using  $\chi(C) = 2 - 2g(C)$ ). Starting from dimension two on, this becomes more subtle.

**Example 15.** *In our example which we have been treating throughout this article, we are dealing with a surface in a three-dimensional ambient space. So the only further Euler characteristics which need to be determined are those of the exceptional divisors themselves. At the moment of birth of an exceptional divisor, it will either be a  $\mathbb{P}^2$  with Euler characteristic 3 or a  $\mathbb{P}^1 \times C$  (for a one-dimensional center  $C$ ) leading to Euler characteristic  $4 - 4g(C)$ . Under subsequent blow-ups the tracking of the changes to the Euler characteristic is then no difficult task.*

```
// compute the topological zeta-function for our isolated
// surface singularity (global and local zeta-function coincide)
> zetaDL(L,1); // global zeta-function
[1]:
(s+6)/(5s2+11s+6)

> zetaDL(L,1,"local"); // local zeta-function
Local Case: Assuming that no (!) charts were dropped
during calculation of the resolution (option "A")
[1]:
(s+6)/(5s2+11s+6)

// zetaDL also computes the characteristic polynomial
// of the monodromy, if additional parameter "A" is given
> zetaDL(L,1,"A");
Computing global zeta function
[1]:
(s+6)/(5s2+11s+6)
[2]:
(s4+s3+s2+s+1)
```

#### 4. DESINGULARIZATION IN EXPERIMENTS

The previous section showed some examples in which desingularization was a crucial step in the calculation of certain invariants and was hence used as a theoretical and practical tool. We now turn our interest to a different kind of settings: experiments on open questions which involve desingularization. Here we only sketch two such topics and the way one could experiment in the respective setting.<sup>7</sup>

**4.1. Bernstein-Sato polynomials.** In the early 1970s J. Bernstein [4] and M. Sato [27] independently defined an object in the theory of D-modules, which is nowadays called the Bernstein-Sato polynomial. The roots of such polynomials have a close, but still somewhat mysterious relation to the multiplicities of exceptional divisors

---

<sup>7</sup>Neither of the two topics should be seen as a suggestion for a short term research project! Both questions, however, might gain new insights from someone playing around with such experiments just for a short while and stumbling into examples which open up new perspectives, insight or conjectures.

in a related desingularization. For briefly recalling the definition of Bernstein-Sato polynomials, we shall follow the article of Kashiwara [21], which also introduces this relation. After that we sketch what computer algebra tools are available in SINGULAR for experiments on this topic.

**Definition 16.** *Let  $f$  be an analytic function defined on some complex manifold  $X$  of dimension  $n$  and let  $\mathcal{D}$  be the sheaf of differential operators of finite order on  $X$ . The polynomials in an additional variable  $s$  satisfying*

$$b(s)f^s \in \mathcal{D}[s]f^{s+1}$$

*form an ideal. A generator of this ideal is called the Bernstein-Sato polynomial and denoted by  $b_f(s)$ .*

Kashiwara then proves the rationality of the roots of the Bernstein-Sato polynomial by using Hironaka's desingularization theorem in the following way:

**Theorem 17** ([21]). *Let  $f$  be as above and consider a blow-up  $F : X' \rightarrow X$  and a new function  $f' = f \circ F$ . Then  $b_f(s)$  is a divisor of  $\prod_{k=0}^N b_{f'}(s+k)$  for a sufficiently large  $N$ .*

More precisely, a principalization of the ideal generated by  $f$  leads to a polynomial  $f' = \prod_{i=1}^m m_i t_i^{r_i}$  with a local system of coordinates  $t_1, \dots, t_m$ . For  $f'$  the Bernstein-Sato polynomial is known to be

$$b_{f'}(s) = \prod_{i=1}^m \prod_{k=1}^{r_i} (r_i s + k).$$

Therefore the roots of the Bernstein-Sato polynomial are negative rational numbers of the form  $-\frac{k}{r_i}$  with exceptional multiplicities  $r_i$  and  $1 \leq k \leq r_i$ . Yet it is not clear at all whether there are any rules or patterns which exceptional multiplicities  $r_i$  actually appear as denominators of roots of the Bernstein-Sato polynomial. (As a sideremark: If this were known, then such knowledge could be used to speed up computations of Bernstein-Sato polynomials whenever a desingularization is known.)

Today there are implemented algorithms for computing the Bernstein-Sato polynomial of a given  $f$  available: by Ucha and Castro-Jiminez [29], Andres, Levandovskyy and Martin-Morales [1] and by Berkesh and Leykin [3]. All of these algorithms do not use desingularization techniques, but rather rely on Gröbner-Bases and annihilator computations. The computed objects, however, are also used (theoretically and in examples) in the context of multiplier ideals and thus have relation to invariants like the log-canonical threshold.

Given algorithmic ways to independently compute the Bernstein-Sato polynomial and the exceptional multiplicities, one could now revisit the exploration of the interplay between these and try to spot patterns to get a better understanding.

**4.2. Positive Characteristic.** Desingularization in positive characteristic is one of the long standing, central open problems in algebraic geometry. In dimensions up to three there is a positive answer (see e.g. [9], [10]), but in the general case there are several different approaches (e.g. [20], [30], [18]) each of which has run

into obstacles which are currently not resolved.

About a decade ago, Hauser started studying the reasons why Hironaka's approach of characteristic zero fails in positive characteristic [17]. Among other findings, he singled out two central points which break down:

- (1) failure of maximal contact:

Hypersurfaces of maximal contact are central to the descent in ambient dimension which in turn is the key to finding the correct centers for blowing up. In positive characteristic, it is well known that hypersurfaces of maximal contact need not exist; allowing hypersurfaces satisfying only slightly weaker conditions is one of the central steps in the approach of Hauser and Wagner for dimension 2 [18]. (For higher dimensions this definition requires a little bit more care [14].)

- (2) increase of order of coefficient ideal:

As the improvement of the singularities is measured by the decrease of the order and of orders for further auxiliary ideals constructed by means of descent in ambient dimension, it is crucial for the proof of termination of resolution that these orders cannot increase under blowing up. Unfortunately this does no longer hold for the orders of the auxiliary ideals in positive characteristic as has again been known since the 1970s. Hauser characterized the structure of polynomials which can exhibit such behaviour in [17].

Although problems of desingularization in positive characteristic are known, this knowledge seems to be not yet broad enough to provide sufficient feedback for suitable modification of one of the approaches to overcome the respective obstacles. Experiments could prove to be helpful to open up a new point of view. In particular, the approach of Hauser and Wagner for surfaces is sufficiently close to the characteristic zero approach of Hironaka (and hence to algorithmic approaches like the one of Villamayor) to allow modification of an existing implementation to provide a tool for a structured search for examples with special properties also in higher dimensions. This has e.g. been pursued in [14].

## REFERENCES

- [1] Andres,D., Levandovskyy,V., Martin-Morales,J.:*Principal Intersection and Bernstein-Sato Polynomial of an Affine Variety*, arXiv:1002.3644
- [2] Beck,T.:*Formal Desingularization of surfaces – the Jung Method revisited*, J.Symb.Comp. **44** (2) (2009), 131–160
- [3] Berkesch,C., Leykin,A.:*Algorithms for Bernstein-Sato polynomials and multiplier ideals*, arXiv:1002.1475
- [4] Bernstein,I.N.:*Teh analytic continuation of generalized functions with respect to a parameter*. Func.Anal.Appl. **6** (1972), 26–40
- [5] Bierstone,E., Milman,P.:*Canonical Desingularization in Characteristic Zero by Blowing up the Maximum Strata of a Local Invariant*, Invent.Math. **128** (1997), 207–302
- [6] Bierstone,E., Milman,P.:*Desingularization of Toric and Binomial Ideals*, J. Alg. Geom. **15** (2006), pp. 443–486
- [7] Blanco, R.:*Desingularization of binomial varieties in arbitrary characteristic*, arXiv:0902.2887v2 and arXiv:1009.0636
- [8] Bravo,A., Encinas,S., Villamayor,O.:*A Simplified Proof of Desingularisation and Applications*, Rev. Math. Iberoamericana **21** (2005), 349–458.
- [9] Cossart,V., Piltant,O.: *Resolution of singularities of Threefolds in positive Characteristic I*, J. Algebra **320** (2008), 1051–1082

- [10] Cossart, V., Piltant, O.: *Resolution of singularities of Threefolds in positive Characteristic II*, J. Algebra **321** (2009), 1836–1976
- [11] Decker, W., Greuel, G.-M., Pfister, G., Schönemann, H.: SINGULAR 3-1-6 — A computer algebra system for polynomial computations. <http://www.singular.uni-kl.de> (2012).
- [12] Denef, J., Loeser, F.: *Caractéristiques de Euler-Poincaré, fonctions zeta locales, et modifications analytiques*, J. Amer. Math. Soc. **4** (1992), pp. 705–720
- [13] Encinas, S., Hauser, H.: *Strong resolution of singularities in characteristic zero*, Comment. Math. Helv. **77** (2002), 821–845.
- [14] Frühbis-Krüger, A.: *A short note on Hauser’s Kangaroo phenomena and weak maximal contact in higher dimensions*, J.Sing. **2** (2010), 128–142
- [15] Fulton, W.: *Introduction to Toric Varieties*, Princeton University Press (1993)
- [16] Hartshorne, R.: *Algebraic Geometry*, Springer (1977)
- [17] Hauser, H.: *Why the characteristic zero proof of resolution fails in positive characteristic* Manuscript 2003, available at [www.hh.hauser.cc](http://www.hh.hauser.cc)
- [18] Hauser, H., Wagner, D.: *Alternative invariants for the embedded resolution of surfaces in positive characteristic*. Preprint 2009.
- [19] Jung, H.: *Darstellung der Funktionen eines algebraischen Körpers zweier unabhängiger Veränderlicher  $x, y$  in der Umgebung einer Stelle  $x=a, y=b$* , J.Reine Angew. Math. **133** (1908), pp. 289–314
- [20] Kawanoue, H.: *Toward resolution of singularities over a field of positive characteristic I*. Publ. Res. Inst. Math. Sci. **43** (2007), 819–909
- [21] Kashiwara, M.: *B-Functions and Holonomic Systems*, Inv. Math. **38** (1976), 33–53
- [22] Lazarsfeld, R.: *Positivity in Algebraic Geometry II*, Springer Berlin (2004)
- [23] Lin, S.: *Algebraic Methods for Evaluating Integrals in Bayesian Statistics*, Ph.D. dissertation, University of California, Berkeley (2011)
- [24] Lipman, J.: *Desingularization of two-dimensional schemes*, Ann.Math. (2) **107** (1978), pp. 151–207
- [25] Mustata, M.: *IMPANGA lecture notes on log canonical thresholds*, arXiv:1107.2676
- [26] Saito, M.: *On real log canonical thresholds* arXiv:0707.2308
- [27] Sato, M., Shintani, T.: *On zeta functions associated with prehomogeneous vector spaces* Annals of Math. **100** (1974), 131–170
- [28] Tian, G.: *On Kähler-Einstein metrics on certain Kähler manifolds with  $c_1(M) > 0$* , Invent.Math. **89** (1997), 225–246
- [29] Ucha, J.M., Castro-Jimenez, F.J.: *Bernstein-Sato ideals associated to polynomials*, J. Symbolic Comput. **37** (5) (2004), 629–639
- [30] Villamayor, O.: *Elimination with applications to singularities in positive characteristic*, Publ. Res. Inst. Math. Sci. **44** (2008), 661–697

INSTITUT FÜR ALGEBRAISCHE GEOMETRIE, LEIBNIZ UNIVERSITÄT HANNOVER, GERMANY